

# **Thermodynamic properties of lithium chloride ammonia complexes for application in a high-lift high temperature chemical heat pump**

**W.G. Haije, E.R.T. Bevers, P.J. van Ekeren**

# THERMODYNAMIC PROPERTIES OF LITHIUM CHLORIDE AMMONIA COMPLEXES FOR APPLICATION IN A HIGH-LIFT HIGH TEMPERATURE CHEMICAL HEAT PUMP

E. R. T. Bevers<sup>1\*</sup>, P. J. van Ekeren<sup>1</sup>, W. G. Haije<sup>2</sup> and H. A. J. Oonk<sup>1</sup>

<sup>1</sup>Chemical Thermodynamics Group, Department of Chemistry, Utrecht University, Padualaan 8  
3584 CH Utrecht, The Netherlands

<sup>2</sup>Energy research Centre of the Netherlands, Energy Efficiency in Industry (EEI), P.O. Box 1, 1755 ZG Petten, The Netherlands

Ammonia absorption by and desorption from lithium chloride at different pressures has been studied using high-pressure differential scanning calorimetry, for application in a high-lift high temperature chemical heat pump. The measurements were performed under isobaric as well as under isothermal circumstances. Clausius–Clapeyron plots were constructed and used to calculate the thermodynamic parameters and to determine the stability regions of the different complexes. Controversies in literature as to the real existing phases are resolved.

**Keywords:** ammonia, chemical heat pump, DSC, lithium chloride, thermodynamic properties

## Introduction

Because the world's oil and gas resources are limited and because of environmental problems associated with their use, one becomes more and more aware of the fact that the use of these resources must be reduced. This may be achieved by (a combination of) the following options:

- make more use of sustainable energy resources, such as solar energy, wind energy, bio energy
- use current resources more efficiently

That there still are significant possibilities to use energy resources more efficiently can be learned from many recent studies. As an example, Spoelstra *et al.* reported that in the Netherlands industrial waste heat in the order of 110 PJ (i.e.  $110 \cdot 10^{15}$  J) per year is actively cooled and dissipated into the environment [1].

Unfortunately, this enormous amount of heat is available at a temperature range of 50 to 150°C, whereas heat that is useful for industrial purposes must be available at a temperature of about 230°C (middle pressure steam).

Lifting heat to a desired high temperature can be done either with a conventional compression heat pump at the expense of a substantial amount of primary energy or with a chemical heat pump (CHP).

In a CHP the high temperature lift is realized by chemical reactions, in particular the absorption of a vapour in a solid. For a specific application the solid-vapour pairs must be carefully selected and characterized. The advantage of a CHP over a compression HP lies in the fact that it can be 'fuelled' with

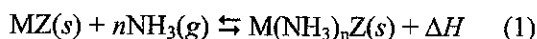
industrial waste heat with a typical efficiency of about 35% thus leading to significant energy and CO<sub>2</sub> emission savings.

The working principle of a CHP has been described extensively by Spoelstra *et al.* [1], and by Wongsuwan *et al.* [2]; in brief, it is as follows. A CHP always uses two carefully selected materials [1, 2], a low temperature salt (LTS, which occasionally may also be replaced by an evaporating fluid like water or ammonia) and a high temperature salt (HTS) that are contained in separate reactors. The reactors are connected to each other so that gas can flow between them in a cyclic process. The HTS complex is decomposed by using available waste heat at medium temperature. The formed gas flows to the reactor containing the LTS. There, a complex of the LTS is formed under release of heat at low temperature. When these reactions, both at a relatively low pressure, are more or less complete, the temperature of the reactor containing the complex of the LTS is increased from low temperature to medium temperature and available waste heat at medium temperature is used to decompose the complex. Now the formed gas flows to the reactor containing the HTS, where it is used for the formation of a complex of the HTS under the release of heat at high temperature. Upon completion of these reactions, that both take place at a relatively high pressure, the temperature of the reactor containing the complex of the HTS is decreased from high temperature to medium temperature, which completes the cycle.

The work described in this paper is part of a research project on the design of a CHP based on the

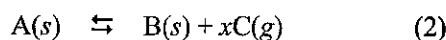
\* Author for correspondence: E.R.T.Bevers@chem.uu.nl

formation and decomposition of (solid) ammonia complexes, according to the general reaction:



From many different working couples, collected and tabulated by Bonnefoi [3], the couples of magnesium chloride and lithium chloride with ammonia appear to be promising, because their transitions are in the right  $p$ - $T$  area and the potential temperature lift is sufficient.

In terms of equilibrium thermodynamics, the equilibrium pressure of the monovariant heterogeneous equilibrium



is the solution of the equation

$$\Delta_r G(T) = \Delta_r G^0(T) + xRT \ln \frac{p(T)}{p_0} = 0 \quad (3)$$

where  $\Delta G$  is the molar Gibbs energy change of the reaction,  $p_0$  a reference pressure,  $\Delta G^0$  the Gibbs energy change at  $p_0$ , and  $R$  the gas constant ( $R=8.3144472 \text{ mol}^{-1} \text{ K}^{-1}$ ). From this equation, taking into account that  $\Delta_r G^0 = \Delta_r H^0 - T\Delta_r S^0$ , where  $H$  stands for enthalpy and  $S$  for entropy, it follows that

$$\ln \frac{p(T)}{p_0} = - \left( \frac{\Delta_r H^0}{xR} \right) \left( \frac{1}{T} \right) + \frac{\Delta_r S^0(T)}{xR} \quad (4)$$

Equilibrium pressures, as a rule, are represented in a Clausius–Clapeyron [3] diagram, where the logarithm of pressure is plotted vs. reciprocal temperature. The slope of the line in the diagram equals to minus the enthalpy effect of the reaction per mole of C divided by the gas constant.

Under the process conditions used for our experiments, the  $pT$  relationships of the formation reaction and those of the decomposition reaction, as a rule, do not coincide. In the Clausius–Clapeyron representation, as a result, there are two lines; one for the formation and one for the decomposition, Fig. 1. The width of the area between the lines, referred to as the area of pseudo-equilibrium [4–6], depends on the cooling/heating rate ( $\beta$ ) of the experiment. The lower the cooling or heating rate is taken, the smaller the pseudo-equilibrium area becomes and the closer the real thermodynamic equilibrium is approached.

Trudel *et al.* [6] adduce two possible reasons for the explanation of this pseudo-equilibrium hysteresis. The first is related to the expansion and contraction of the crystal lattice as the ammonia content in the material changes: the hysteresis may be caused by an activation barrier necessary to expand the material (work of expansion that is not recovered on contraction). The second explanation of the observed hysteresis can be found in the fact that there could be a tempera-

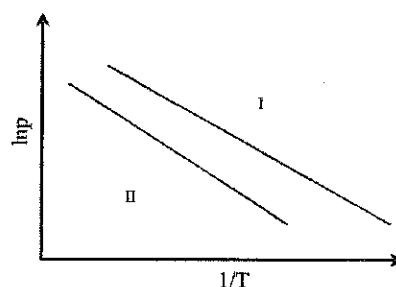


Fig. 1 Clausius–Clapeyron representation of the pressure–temperature relationships under the process circumstances of our experiments, showing an area of pseudo-equilibrium between formation (I) and decomposition (II)

ture difference between the gas and the crystalline complex caused by the (exothermic/endothermic) heat effect of the reaction.

The results presented in this paper pertain to the complexes formed between LiCl and  $NH_3$ . The formation of these complexes, for pressures up to about 1 bar, has been studied by Bonnefoi [7], and by Collins and Cameron [8]. Bonnefoi reported the formation of a stable di-ammonia complex; a result that could not be confirmed by Collins. In our study, we applied pressures from 1 to 5 bar, and used high-pressure differential scanning calorimetry (HPDSC) to measure the heat effects and the  $pT$  relationships of the formation and decomposition reactions. In the CHP under development, LiCl is the low temperature salt, and  $MgCl_2$  the high temperature salt. The results obtained for the complexes formed by  $MgCl_2$  and ammonia are the subject of a forthcoming paper.

## Experimental

### Materials and methods

#### Sample preparation

Lithium chloride (Merck, 99.0%) was used as starting material. Because lithium chloride is hygroscopic, the sample was weighed and then dehydrated in a Mettler-Toledo DSC821°. After dehydration the sample was quickly weighed again to determine the amount of anhydrous lithium chloride. Then the sample was introduced into the HPDSC cell and heated again because between weighing and introducing it may have slightly hydrated. The atmosphere was nitrogen (obtained by the vaporization of liquid nitrogen, negligible impurity, Hoekloos) so that the small amount of water absorbed by the sample was able to evaporate. The uncertainty in the sample mass (including the balance-error) is approximately 2.5%. After heating up, the atmosphere was changed from nitrogen to ammo-

nia (Hoekloos, ammonia purity higher than 99.98%). At this point the sample was ready to be measured.

### Thermal analysis

The HPDSC used for the measurements was a Mettler-Toledo DSC27HP, which has a maximum working temperature of 600°C and a maximum working pressure of 70 bar. The cooling was vested by streaming cold water.

The system was calibrated prior the measurements, using indium, tin and lead. It was interesting that we found that the temperature calibration parameters depend on pressure [9]. It is quite well possible that, for a change involving gases and unlike the melting of a metal, the heat regulation inside the sample container is such that the heat effect is not measured to its full extent. In terms of experimentation this is an important issue; it will be readdressed in the discussion part of this paper.

The calibration and measurements were performed using 40  $\mu\text{L}$  golden pans with a pierced lid, in ammonia atmosphere. An empty pan was used as reference. To avoid inaccuracies arising from mass or heat transfer only a few milligrams of salt was used.

The pressure and gas flow in the cell were controlled by Brooks Instruments pressure and flow controllers, type 5866 and 5850S, respectively. During the measurements, the DSC cell was purged with ammonia gas at a constant rate of 50  $\text{mL min}^{-1}$ .

### Experimental procedure

Two types of measurements were performed. In the first method the temperature was changed at constant pressure (isobaric), in the second method the pressure was changed at constant temperature (isothermal). Both measurements were used to determine the transitions from phase A to B.

#### Scanning temperature (isobaric)

This method was performed to determine the position of the solid-gas equilibrium lines. For a constant pressure the sample was submitted to an increasing or decreasing temperature at a rate of 1.0  $\text{K min}^{-1}$  (Fig. 2).

#### Scanning pressure (isothermal)

The procedure used for the formation (Fig. 3) was to carefully bring the system to the correct pressure and temperature to arrive at the starting situation (point A). From point A the temperature was decreased to point B. After stabilization at point B the pressure was very slowly changed downwards with steps of 0.01 bar towards point C until a thermal effect was observed.

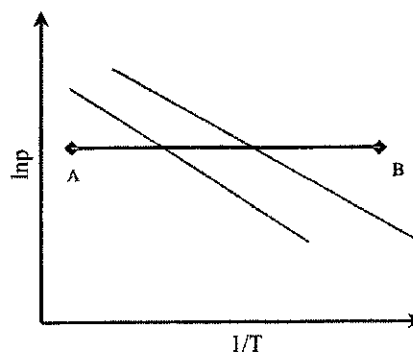


Fig. 2 Principle of experimental scanning temperature method in Clausius-Clapeyron's diagram

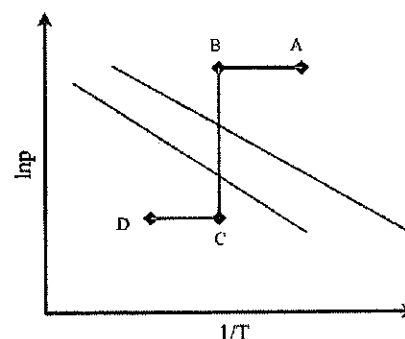


Fig. 3 Principle of experimental scanning pressure method in Clausius-Clapeyron's diagram

This way the (pseudo)equilibrium was found. For the decomposition the route D, C, B was followed.

## Results and discussion

### Scanning temperature method

For a given  $\text{NH}_3$  pressure, the sample is subjected to a temperature program, such that the range from 298.15 to 423.15 K is passed three times, forth and back. Figure 4 represents a typical example of the results of this method. On heating as well as on cooling three effects were observed, corresponding to decomposition and formation reactions, respectively. The middle thermal effect is rather large compared to the other two.

The three reactions, at this place, are represented by the following equations:



The thermal effect at high temperature is caused by the transition between the pure LiCl into the complex containing the lowest amount of  $\text{NH}_3$ . The low temperature transition involves one molecule of  $\text{NH}_3$  (reaction (5)). The middle temperature transition in-

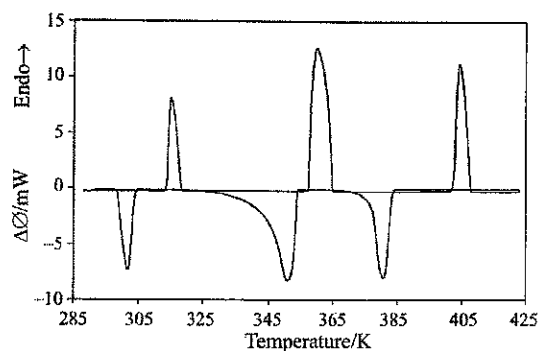


Fig. 4 Typical example of the transitions of LiCl and NH<sub>3</sub> at  $p=3.0$  bar

cludes a certain number ( $\alpha$ ) of molecules NH<sub>3</sub> (reaction (6)) and the high temperature transition includes  $(3-\alpha)$  molecules NH<sub>3</sub> (reaction (7)). The literature [3, 7, 8] is univocal of the existence of reaction (5), which is therefore assumed to be correct.

The results of all the transitions at different pressure are given in Table 1 and are plotted in a Clausius–Clapeyron diagram (Fig. 5). Note that the

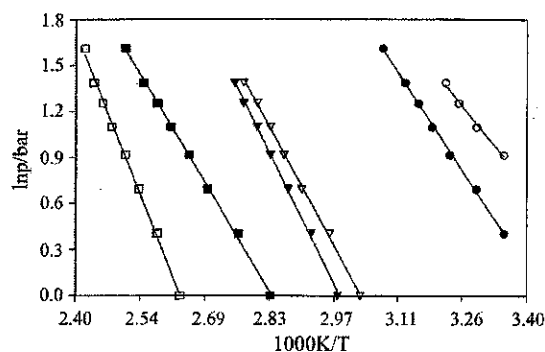


Fig. 5 Results of the low temperature transition of LiCl:  $\circ$  – formation,  $\bullet$  – decomposition; the middle temperature transition:  $\nabla$  – formation,  $\blacktriangledown$  – decomposition and the high temperature transition:  $\blacksquare$  – formation,  $\square$  – decomposition

heat of transition, as measured by the HPDSC, is given with respect to 1 g of lithium chloride.

It is noteworthy that during the first runs the heat of transition is lower compared to the effect measured in the subsequent runs. A plausible reason of this phenomenon is that, the first time the LiCl expands, due to the absorption of ammonia, it is transforming into smaller

Table 1 Experimental results of all transitions of lithium chloride

Low temperature transition					
Formation			Decomposition		
Pressure/bar	Transition temperature/K	$-Q/J\ g^{-1}$	Transition temperature/K	$Q/J\ g^{-1}$	Number of measurements
1.50	–	–	298.36	599	3*
2.00	–	–	304.37	548	6**
2.50	298.55	619	309.57	612	6
3.00	303.88	631	313.51	631	6
3.50	307.46	614	316.77	614	4
4.00	310.41	648	319.89	643	6
5.00	–	–	324.50	603	4*
Middle temperature transition					
Formation			Decomposition		
Pressure/bar	Transition temperature/K	$-Q/J\ g^{-1}$	Transition temperature/K	$Q/J\ g^{-1}$	Number of measurements
1.00	329.58	1638	335.09	1743	6
1.50	337.69	1663	342.57	1721	6
2.00	344.24	1523	348.74	1584	6**
2.50	349.40	1712	353.42	1726	6
3.00	353.78	1830	357.32	1805	6
3.50	357.40	1771	360.58	1724	4
4.00	360.85	1865	363.48	1800	6
High temperature transition					
Formation			Decomposition		
Pressure/bar	Transition temperature/K	$-Q/J\ g^{-1}$	Transition temperature/K	$Q/J\ g^{-1}$	Number of measurements
1.00	352.83	901	379.59	935	6
1.50	362.92	901	387.39	927	6
2.00	371.32	854	393.56	885	6**
2.50	377.85	927	398.43	933	6
3.00	383.35	972	402.51	974	6
3.50	387.98	926	406.07	929	4
4.00	392.23	958	409.60	966	6
5.00	398.86	943	413.69	987	4

\*Due to lack of cooling power only the decomposition was observed, \*\*first measurement with sample

and smaller crystals. After five completed cycles the heat of transition does not change any more. For that matter, the number of measurements given in Table 1, pertain to the number of cycles from the sixth cycle on.

The heat effects and the temperatures of the transitions, evaluated from the measured curves and displayed in Table 1, are the mean values for the number of measurements given in the last column of the table.

In detail, taking the 3 bar case of the middle temperature reaction, the experimental recordings are as follows. The temperatures reported for the reactions are the extrapolated onset temperatures of the peaks. For the formation reaction the onset temperatures of the six experiments range from 353.76 to 353.80 K, the mean value being 353.78 K with a standard deviation of 0.012 K. This high instrumental precision justifies the use of two decimal places for the temperature. For the decomposition reaction the onset temperatures are from 357.29 to 357.35 K, the mean value being  $357.32 \pm 0.02$  K. The individual heat effects range from 1819 to 1838  $\text{J g}^{-1}$ , for the formation reaction, and from 1802 to 1814  $\text{J g}^{-1}$  for the decomposition reaction. The mean values are given by  $1830 \pm 9$  and  $1805 \pm 5$   $\text{J g}^{-1}$ , respectively. In view of the standard deviations, the heat effects in Table 1 are given as integers in  $\text{J g}^{-1}$ .

Enthalpy and entropy effects derived from the experimental data in terms of Eq. (4), or, in other terms, derived from the Clausius–Clapeyron plots, are given in Table 2. To calculate, for given pressure, the temperature with a precision of 0.01 K,  $\Delta H$  must be given as an integer in  $\text{J mol}^{-1}$  and  $\Delta S$  in two decimal places.

At pressures over 4.0 bar, the middle temperature transition behaved differently. The thermal effect of the transition divides into two smaller thermal effects (Fig. 6). This behaviour of the complex suggests that more than one molecule of  $\text{NH}_3$  is involved in this reaction. Due to the lack of cooling power, the low temperature formation (the one with the most  $\text{NH}_3$  molecules) had to be established during a longer time at room temperature. Therefore it is not visible in this figure.

#### Scanning pressure method

Isothermal measurements were carried out for the middle temperature transition at three different tem-

**Table 2** Enthalpy and entropy changes derived from the experimental data in terms of Eq. (4)

Transition		$\Delta H/$ $\text{J mol}^{-1}$	$\Delta S/$ $\text{J K}^{-1} \text{mol}^{-1}$
Low temperature	formation	30431	109.44
	decomposition	36790	126.59
Middle temperature	formation	43681	132.62
	decomposition	49098	146.58
High temperature	formation	40470	114.76
	decomposition	60494	159.43

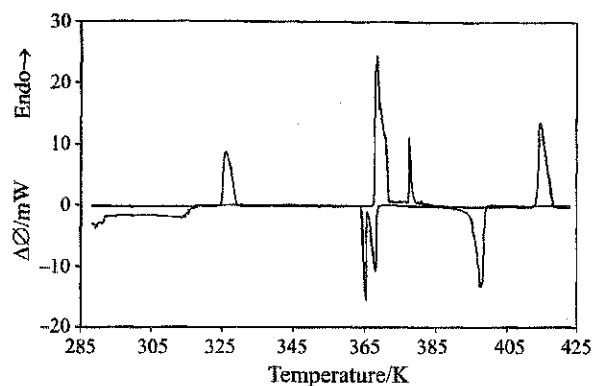


**Fig. 6** Example of the splitting up of the thermal effect at  $p=5.0$  bar

peratures, namely 356.40, 345.65 and 337.15 K. These temperatures were rather arbitrarily chosen; the pressures to apply were estimated from the scanning temperature method. A typical example of the collected HPDSC curve at 345.65 K is given in Fig. 7. During this measurement the pressure was stepwise decreased from the starting pressure of 1.94 bar. After each step of 0.01 bar there was a waiting time imposed of fifteen minutes. In the diagram it is visible that around 6700 s (point a) an endothermic effect started, which is at a pressure of 1.87 bar, corresponding to the decomposition of the tri-ammonia lithium chloride complex. At point b the pressure was again decreased by 0.01 bar. At point c there was a pressure drop of 0.55 bar to accelerate the reaction, which results in the large endothermic effect.

The results obtained by the scanning pressure method are summarized in Table 3.

The  $\Delta H$  and  $\Delta S$  values derived from the Clausius–Clapeyron plot are given in Table 4.

When the results of the scanning temperature and the scanning pressure method are plotted in one diagram (Fig. 8) it becomes obvious that by the scanning pressure method the pseudo-equilibrium area is smaller than by using the scanning temperature method

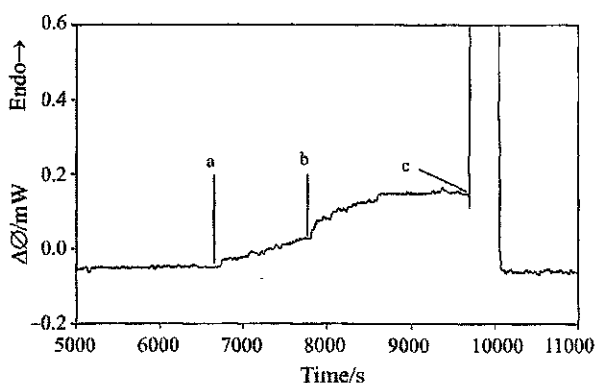


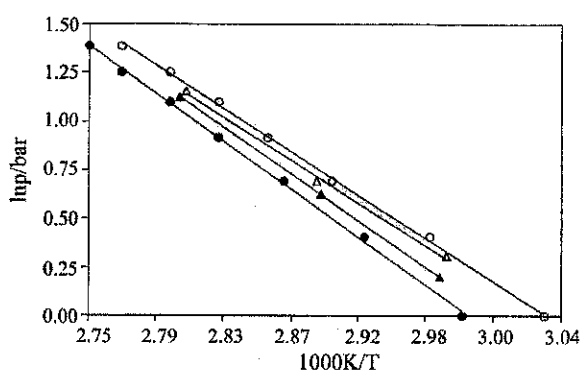
**Fig. 7** Example of the obtained results of the scanning pressure method

**Table 3** Summary of the transition temperatures obtained by the scanning pressure method

Middle temperature transition		
	formation	decomposition
Transition temperature/K	pressure/bar	pressure/bar
356.40	3.17	3.08
345.65	2.00	1.87
337.15	1.36	1.22

**Table 4** Enthalpy and entropy effects derived from Fig. 8 in terms of Eq. (4)

Middle temperature	$\Delta H/\text{J mol}^{-1}$	$\Delta S/\text{J K}^{-1} \text{mol}^{-1}$
Formation	43919	132.82
Decomposition	48046	144.18

**Fig. 8** Results of the middle temperature transition from both the scanning temperature method,  $\circ$  – formation,  $\bullet$  – decomposition and the scanning pressure method,  $\triangle$  – formation,  $\blacktriangle$  – decomposition

for determining the transitions. This implies that by using the scanning pressure method a better approach of the thermodynamic equilibrium is established.

Note that the enthalpy effect obtained by HPDSC is calculated with respect to one mole of LiCl; in contrast to the effect derived from the Clausius–Clapeyron diagram, which is with respect to one mole of  $\text{NH}_3$ .

**Table 5** Survey of the numerical outcome of our investigation

Transition		Average $Q/\text{J g}^{-1}$	$\Delta H$ from HPDSC curve/ $\text{kJ mol}^{-1}$	$\Delta H$ from C–C diagram/ $\text{J mol}^{-1}$	$\Delta S$ from C–C diagram/ $\text{J K}^{-1} \text{mol}^{-1}$
Low temperature	formation	$-628 \pm 15$	$-26.4 \pm 0.6$	30431	109.44
	decomposition	$617 \pm 17$	$25.9 \pm 0.7$	36792	126.60
Middle temperature*	formation	$-1746 \pm 91$	$-73.4 \pm 3.8$	43681	132.62
	decomposition	$1753 \pm 39$	$73.7 \pm 1.6$	49098	146.58
Middle temperature**	formation	–	–	43919	132.82
	decomposition	–	–	44208	132.89
High temperature	formation	$-932 \pm 28$	$-39.2 \pm 1.2$	40470	114.76
	decomposition	$950 \pm 26$	$39.9 \pm 1.1$	60494	159.43

\*‘scanning temperature method’, \*\*‘scanning pressure method’

A survey of the numerical results of our investigation is presented in Table 5. For each of the reactions, the directly measured heat effects are the mean of the corresponding data in Table 1, leaving out the data for the experiments labelled in Table 1 with two asterisks.

From an inspection of the numerical information in Table 5, and as a first step concentrating on the low- and high temperature reactions, the following conclusions can be drawn. First of all, and not unexpected, the enthalpy values obtained by direct measurement (HPDSC) differ from the ones derived from Clausius–Clapeyron (C–C) plots, and so to a different extent for formation and decomposition. In an internally consistent manner, the C–C values for formation are about 1.1 times higher than the direct ones; and the C–C values for decomposition about 1.4 times.

Making consideration for the ratios of the heat effects, derived from C–C plots/directly obtained, the direct heat effect of the middle reaction is about two times the value derived from the C–C plots. The importance of this observation is that the number of  $\text{NH}_3$  molecules involved in the middle reaction is equal to twice the number of molecules in the two other reactions. In other words, the experimental results support the conclusion that in the low temperature reaction the tetra complex changes to the tri-ammonia complex; next, in the middle reaction, the tri complex to the mono complex; and, finally, in the high temperature reaction, the mono complex changes into  $\text{NH}_3$  plus pure LiCl.

Bonnefoi [7] observed not only the formation of the mono-, tri-, and tetra-ammonia complexes, but also the formation of the di-ammonia complex. We observed the splitting up of the middle peak at pressures above about 4 bar, Fig. 6, which indicates the existence of a fourth stable ammonia-complex, possible the di-ammonia complex. The heat effects reported by Bonnefoi, taking the sum of the effects of the two intermediate reactions, show the same trends as the effects measured by us.

Collins and Cameron [8], making reference to the work by Bonnefoi, succeeded in preparing the mono-,

tri- and tetra-ammonia complexes, but could not obtain the di-ammonia complex. In addition, they found that the vapour pressures for the mono complex almost coincide with Bonnefoi's data for the di-complex.

A survey of the available information is presented in Fig. 9. For reasons of clarity, our decomposition data are not included in this figure. Our  $pT$  data for the formation reactions, rather than our data for the decomposition reactions, line up with the equilibrium data by Collins and Cameron. This observation suggests that the formation reactions in the cooling experiments, after passing the equilibrium temperature, are less delayed than the decomposition reactions in the heating experiments.

The explanation of the narrowing down of the pseudo-equilibrium area obtained with the scanning temperature method is found in the fact that the scanning pressure method was performed with steps of 0.01 bar while the scanning temperature method was performed with a heating rate  $1.00 \text{ K min}^{-1}$ . The steps of 0.01 bar per 15 min are commensurable with approximately  $0.005 \text{ K min}^{-1}$ .

It is plausible to assume that, apart from time, the realization of true equilibrium is favoured by circumstances of high temperature and pressure. The fact that the difference in onset temperatures of the decomposition and formation reactions decreases with increasing temperature is in line with this assumption. From the data for the high temperature reaction, for example, it would follow that the delay in the reactions would disappear at about 450 K. Or, in other terms, under the circumstances of our experiments, transitions at equilibrium conditions should be observed at temperatures above 450 K.

For the high temperature reaction the point of intersection of the two straight lines in the  $C-C$  representation is at 448 K and 19.0 bar. In view of the assumption expressed in the preceding paragraph the line of

true equilibrium should pass through this point, and, in addition, run between the lines for the formation and decomposition reactions. For the middle temperature reaction the point of intersection is calculated at 388 K and 11 bar; and for the low temperature reaction 371 K and 27 bar. The curious thing is that the 'equilibrium lines' calculated with the directly measured heats of reaction (evaluated from the peak areas), are running outside the regions enclosed by the lines of formation and decomposition. Owing to the complexity of the system, a simple and straightforward explanation of the disagreement is not easily given. To underline this, we consider the consequences of two extreme assumptions.

In the first assumption the instrument does not measure the heat effect to its full extent, possibly because the gas-solid reaction of the expanded salt has a poor heat conductivity, the true heat effect being in between of the  $C-C$  values for formation and decomposition. When assuming the true heat effect being the mean of these two  $C-C$  values, one can calculate that the heat effect provided by the instrument is equal to 78% of the true effect (in detail for the three reactions, taking into account the factor 2 for the middle temperature reaction, the percentages, from low- to high temperature reaction, are 77.3, 79.3 and 77.6). The validity of the 78% assumption is supported by the fact that virtually full agreement is obtained with the heat effects measured by Bonnefoi by solution calorimetry.

In the second assumption the discord is caused by the (partial) dissociation of ammonia into nitrogen and hydrogen. A fact is, that if the system respects the principle of minimal Gibbs energy, ammonia will be partially dissociated. The degree of dissociation is easily calculated: it runs up from 2%, for conditions of the low temperature formation reaction, to 22% for conditions of the high temperature decomposition reaction. If dissociation of ammonia actually occurs, this implies that the partial ammonia pressure will be smaller than the measured pressures and the heat of dissociation of ammonia (around  $47 \text{ kJ mol}^{-1}$ ) must be taken into account. However Haije and Grisel [10] actively searched for hydrogen and nitrogen as decomposition products over the entire  $pT$ -range, but did not find any indication for significant ammonia dissociation.

During the cycles after the initial ones, the measured temperature/pressure and heat effects remain unchanged. This observation, obviously, is in favour of the selection of LiCl-ammonia complexes for use in a CHP. Clearly the stability region of the di-ammoniate is small enough not to hamper the functioning of the heat pump.

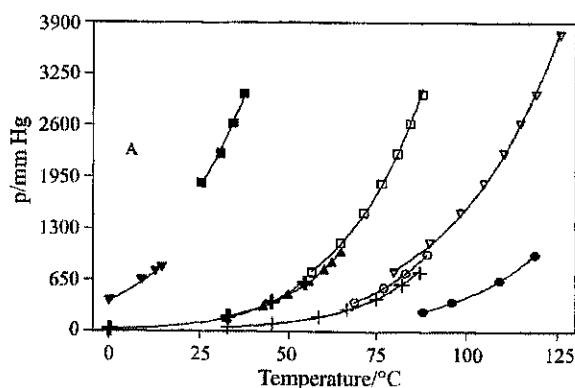
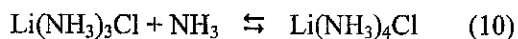
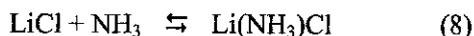


Fig. 9 Combined data originating from  $\nabla, \triangle, \circ, \bullet$  - Bonnefoi,  $+, \times$  - Cameron and Collins and  $\blacksquare, \square, \nabla$  - the formation data represented here. Phase A is uniformly ascribed as  $\text{Li}(\text{NH}_3)_4\text{Cl}$

## Conclusions

The formation and decomposition of complexes formed by LiCl and NH<sub>3</sub> has been studied in a dynamic, scanning manner by means of HPDSC, both in an isobaric and an isothermal mode, the ranges being from 1 to 5 bar in pressure, and from 298 to 425 K in temperature.

Under the applied experimental circumstances with pressures below 4.0 bar, the formation and decomposition of the complexes comprise three chemical reactions:



For the three reactions, the pressure–temperature relationships of the formation reaction are different from those of the decomposition reaction; and such that there are two straight-line relationships in the Clausius–Clapeyron representation.

Above the pressure of 4.0 bar a fourth stable complex is observed, namely the di-ammonia complex.

The pressure–temperature relationships and the heat effects remain unchanged during the number of applied cycles. This implies that the reactions be-

tween LiCl and NH<sub>3</sub> constitute a promising candidate for use as a LTS in a CHP system.

## References

- 1 S. Spoelstra, W. G. Haije and J. W. Dijkstra, *Appl. Therm. Eng.*, 2 (2002) 1619.
- 2 W. Wongsuwan, S. Kumar, P. Neveu and F. Meunier, *Appl. Therm. Eng.*, 21 (2001) 1489.
- 3 Ph. Touzain, Thermodynamic values of ammonia-salts reactions for chemical sorption heat pumps, *Int. Sorption Heat Pump Conf.*, Munich, German, March 1999.
- 4 B. Spinner, *Heat Recovery Systems CHP*, 13 (1993) 301.
- 5 V. Goetz and A. Marty, *Chem. Eng. Sci.*, 47 (1992) 4445.
- 6 J. Trudel, S. Hosatte and M. Ternan, *Appl. Therm. Eng.*, 19 (1999) 495.
- 7 J. Bonnefoi, *Ann. Chim. Phys.*, 23 (1901) 317.
- 8 S. C. Collins and F. K. Cameron, *J. Phys. Chem.*, 32 (1928) 1705.
- 9 P. J. van Ekeren and E. R. T. Bevers, *J. Therm. Anal. Cal.*, to be submitted.
- 10 Private communication with W. G. Haije and R. J. H. Grisel, Energy Research Centre of the Netherlands.

Received: April 21, 2006

Accepted: September 14, 2006

DOI: 10.1007/s10973-006-7666-3